geosciences

MDPI

Article

Trigger Mechanisms of Gas Hydrate Decomposition, Methane Emissions, and Glacier Breakups in Polar Regions as a Result of Tectonic Wave Deformation

Leopold I. Lobkovsky [1,2,3], Alexey A. Baranov [4], Mukamay M. Ramazanov [5,6], Irina S. Vladimirova [1,3], Yurii V. Gabsatarov [1,3], Igor P. Semiletov [2] and Dmitry A. Alekseev [1,2,3,*]

1 P.P. Shirshov Institute of Oceanology, Russian Academy of Sciences, 36 Nakhimovsky Ave., 117997 Moscow, Russia
2 Laboratory of the Joint Research of Land-Shelf Arctic System, National Research Tomsk State University, 36 Leninsky Ave., 634050 Tomsk, Russia
3 Moscow Institute of Physics and Technology (MIPT), 9, Institutskiy Lane, 141700 Dolgoprudny, Russia
4 Institute of Earthquake Prediction Theory and Mathematical Geophysics, Russian Academy of Sciences, 84/32 Profsoyuznaya Str., 117997 Moscow, Russia
5 Institute for Geothermal Research and Renewable Energy—Branch of Joint Institute for High Temperatures, Russian Academy of Sciences, 367032 Makhachkala, Russia
6 Institute of Geosphere Dynamics, Russian Academy of Sciences, 119334 Moscow, Russia
* Correspondence: alexeevgeo@gmail.com

Abstract: Trigger mechanisms are proposed for gas hydrate decomposition, methane emissions, and glacier collapse in polar regions. These mechanisms are due to tectonic deformation waves in the lithosphere–asthenosphere system, caused by large earthquakes in subduction zones, located near the polar regions: the Aleutian arc, closest to the Arctic, and the Antarctica–Chilean and Tonga–Kermadec–Macquarie subduction zones. Disturbances of the lithosphere are transmitted over long distances (of the order of 2000–3000 km and more) at a speed of about 100 km/year. Additional stresses associated with them come to the Arctic and Antarctica several decades after the occurrence of seismic events. On the Arctic shelf, additional stresses destroy the microstructure of metastable gas hydrates located in frozen rocks at shallow depths, releasing the methane trapped in them and leading to filtration and emissions. In West Antarctica, these wave stresses lead to decreases in the adhesions of the covered glaciers with underlying bedrock, sharp accelerations of their sliding into the sea, and fault occurrences, reducing pressure on the underlying rocks containing gas hydrates, which leads to their decomposition and methane emissions.

Keywords: Arctic; West Antarctica; permafrost; metastable gas hydrates; methane emission; glacier collapse; large earthquakes; tectonic deformation waves; Aleutian subduction zone; Chilean and Tonga–Kermadec–Macquarie subduction zones; trigger mechanisms

Citation: Lobkovsky, L.I.; Baranov, A.A.; Ramazanov, M.M.; Vladimirova, I.S.; Gabsatarov, Y.V.; Semiletov, I.P.; Alekseev, D.A. Trigger Mechanisms of Gas Hydrate Decomposition, Methane Emissions, and Glacier Breakups in Polar Regions as a Result of Tectonic Wave Deformation. *Geosciences* **2022**, *12*, 372. https://doi.org/10.3390/geosciences12100372

Academic Editors: Evgeny Chuvilin and Jesus Martinez-Frias

Received: 22 August 2022
Accepted: 2 October 2022
Published: 8 October 2022

1. Introduction

It is known that gas hydrates as solid crystalline substances can exist in sedimentary rocks under certain PT conditions, forming deposits inside the so-called hydrate stability zone (HSZ), which, for example, for Arctic land is located at depths of more than 200 m [1]. However, in reality, gas hydrates are often found higher along the sections of the sedimentary strata of frozen rocks up to the very surface of the Earth, in a metastable state. This state is realized as a result of the manifestation of the effect of self-preservation [2–9], when, in violation of the PT stability conditions, the process of dissociation of the gas hydrate with the release of gas and water quickly stops due to the freezing of water at a negative temperature and the formation of thin ice shells locking the released gas and preventing further decomposition of gas hydrate particles (Figure 1) [10].

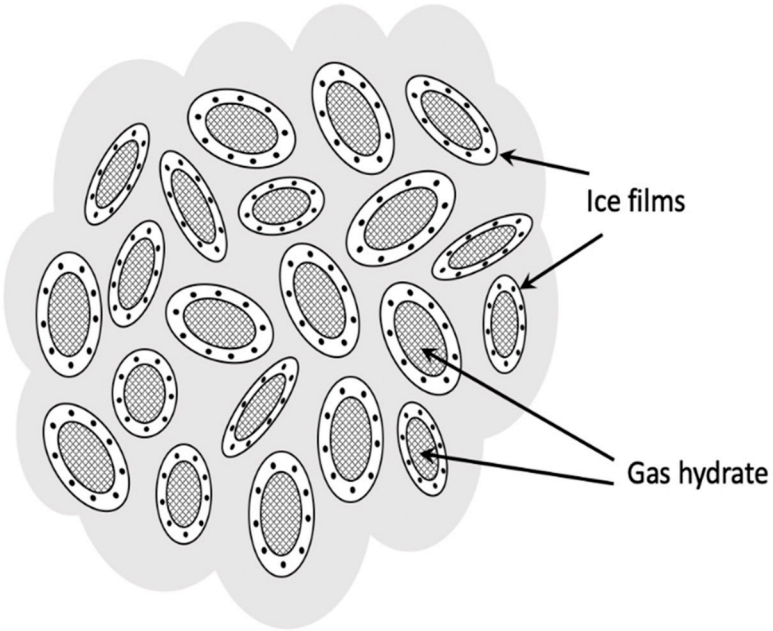

Figure 1. Metastable gas hydrate structure.

The relationship between the gas hydrate stability zone (HSZ) and the zone of possible occurrences of metastable relict gas hydrates (hydrate instability zone, HUZ) in a continental permafrost setting is schematically shown in Figure 2. The depth range of the HSZ includes the lower part of the permafrost zone with a thickness of about 300 m. The HUZ is the portion of the permafrost zone located above the HSZ, where the previously formed hydrates exist due to the self-preservation effect. The evolutionary process of gas hydrate formation in permafrost was studied in a number of works [11–14]. This process, in particular, may be associated with the mechanism of cryogenic gas accumulation, during which the water-dissolved gas is released and accumulated in lithological and permafrost traps within the formations undergoing freezing. Further freezing leads to an increase in pressure in the trapped gas, and part of the gas transforms into hydrate. After the trap becomes completely frozen, the pressure gradually decreases and some part of the hydrate can decompose due to the self-preservation effect, forming a mixed gas accumulation in which free gas and gas hydrates coexist. In some areas of the permafrost zone (Timan–Pechora region, Eastern Siberia, the north of the Russian Far East, as well as areas of northern Canada and Alaska), the formation of hydrates in the upper layers of the frozen rock section could occur during the last glaciation epochs and coastal transgressions of the Arctic Ocean, producing excess pressure within subsurface formations, which contribute to the transition (from the gas to hydrate state). During the ocean regression or glacier retreat, the hydrate-bearing rock could become deposited above the top of the HSZ interval and form a metastable relict gas hydrate, as a result of partial decomposition and the self-preservation effect [1] (Figure 2).

Metastable gas hydrates located close to the surface will be sensitive to small additional stresses caused by various factors, since thin ice shells will collapse under the influence of externally applied stresses, creating opportunities for rapid gas filtration and emission [15–18]. One of the factors creating additional stresses in the lithosphere and its upper sedimentary shell may be tectonic wave deformation in the lithosphere–asthenosphere system, which propagate with velocity in the range of 10–200 km per year [19], i.e., 6 orders of magnitude lower than the velocity of elastic seismic waves and 6 orders of magnitude faster than the speed of movement of lithospheric plates.

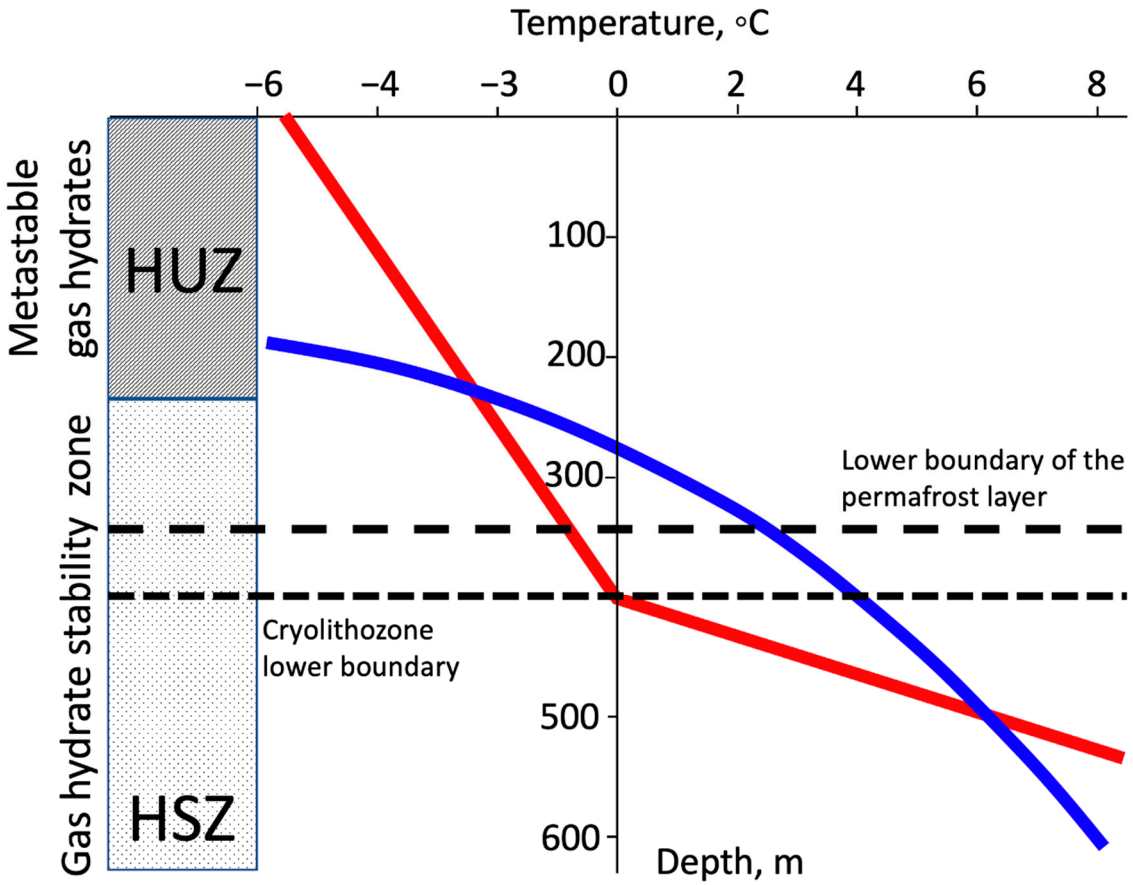

Figure 2. Hydrate stability and metastability zones. The depth-temperature profile is shown by the red line; the blue curve indicates the equilibrium P-T conditions of methane hydrate formation.

It is assumed that a similar trigger mechanism for the destruction of gas hydrates also works in Antarctica, but taking into account the ice covering deeper sedimentary rocks containing gas hydrates. The destruction of these subglacial gas hydrates and the corresponding methane emissions can occur during the destruction of the cover and shelf glaciers, which can be initiated by the trigger mechanism of additional stresses in the lithosphere arising from the arrival of tectonic wave deformation in Antarctica caused by the large earthquakes surrounding the Antarctica–Chilean and Tonga–Kermadec–Macquarie zones.

The geodynamic concept of the trigger mechanisms of the decomposition of gas hydrates, methane emissions, and the destruction of glaciers in the Arctic and Antarctica associated with tectonic wave deformation caused by large earthquakes in the nearest polar regions is considered below.

2. Tectonic Wave Deformation and Trigger Mechanism of Destruction of Gas Hydrates and Methane Emissions in the Arctic

The phenomenon of tectonic wave deformation in the Earth's lithosphere has long attracted the attention of geophysicists, mainly in connection with the observed processes of migration of seismic activity [19–26]. The problem of migration of seismic activity has a half-century history of systematic studies that considered the trigger effects of the occurrences of seismicity as a result of the propagation of deformation waves in the lithosphere. To date, geodetic and hydrological measurements in many regions of the world have revealed the migration of deformations at a rate of about 10–100 km/year [27–31]. The migration of earthquake epicenters coincides in speed (10–100 km/year) and direction with the displacement of crustal deformations [21].

For the first time, a model of the propagation of tectonic stresses in the lithosphere was proposed by V. Elsasser in 1969 [32] to explain the aftershock migration zones after strong earthquakes, considering the one-dimensional problem of the associated horizontal displacements of the elastic lithosphere underlain by a viscous asthenosphere. The resulting diffusion-type equation made it possible to estimate the characteristic diffusion rate of averaged tectonic stresses in the lithosphere, which coincided in the order of magnitude (several tens of km/year) with the observed migration rate of aftershocks. Later, this trend in modern geodynamics and geophysics was widely developed and various models of slow deformation waves in the lithosphere were proposed to describe the migration of earthquakes along island arcs, transform faults, and other tectonic structures [30,33–39].

Recently, the tectonic wave deformation scheme was proposed as a trigger mechanism for the destruction by additional stresses of metastable gas hydrates located in frozen rocks on the Arctic shelf [10]. The consequence of the destruction of gas hydrates is an increase in methane emissions, which can be considered the cause of climate warming in the Arctic. To confirm the proposed trigger hypothesis of the destruction of gas hydrates by deformation waves, it is desirable to have statistical data on the phases of increased methane emissions on the Arctic shelf, timed to tectonic waves, over a sufficiently long time interval. Unfortunately, although direct observations of methane emissions on the Arctic shelf, regularly carried out in marine expeditions of the Russian Academy of Sciences over the last 25 years, have demonstrated intense methane emissions in certain areas of the shelf [40,41], they cannot provide the necessary statistics on changes in total methane emissions on the Arctic shelf during the 20th and 21st centuries. On the other hand, there are good statistics of changes in the temperature of the environment over the past century, which clearly showed the sharp beginning of the phase of the growth of the average temperature in the Arctic in 1979–1980, which continued into the 21st century up to the present day [10]. Regarding deformation waves on the Arctic shelf, it was assumed that they were caused by large earthquakes in the Aleutian subduction zone closest to the Arctic region. Therefore, an argument in favor of the proposed hypothesis could be the existence of a correlation between the time of occurrence of the large earthquakes in the Aleutian Island arc, causing tectonic waves, and the time of the onset of the phase of rapid warming associated with methane emissions. It is easy to make sure that such a correlation exists. If we turn to historical data on seismic events in the Aleutian Arc over the past century, first of all, an unprecedentedly powerful series of three large catastrophic earthquakes that occurred in a short period of time from 1957 to 1965 stands out: the large earthquake of 1957 in the central part of the arc with a magnitude of M = 8.6, the great earthquake of 1964 on the eastern end of the arc with a maximum magnitude of M = 9.3 (Alaska earthquake) and, finally, the late earthquake of 1965 in the western part of the arc with a magnitude of M = 8.7 [10]. As these were large earthquakes with magnitudes greater than 8 that generated tectonic wave deformation, it can be concluded that between the average generation time of tectonic waves in the Aleutian arc and the beginning of a noticeable increase in temperature in the Arctic, there is a time interval of about 20 years, which is naturally explained by the time of propagation of tectonic waves from the Aleutian subduction zone to the Arctic shelf. Taking into account the average distance of about 2000 km between the shelf area and the Aleutian arc and taking the average speed of propagation of tectonic waves (of about 100 km/year), we obtained the delay value of 20 years, which is in favor of the proposed geodynamic scheme of trigger destruction of shelf gas hydrates by tectonic waves from the subduction zone. The scheme of the seismogenic trigger mechanism of methane emission on the shelf due to the destructive effect on gas hydrates is presented in Figure 3.

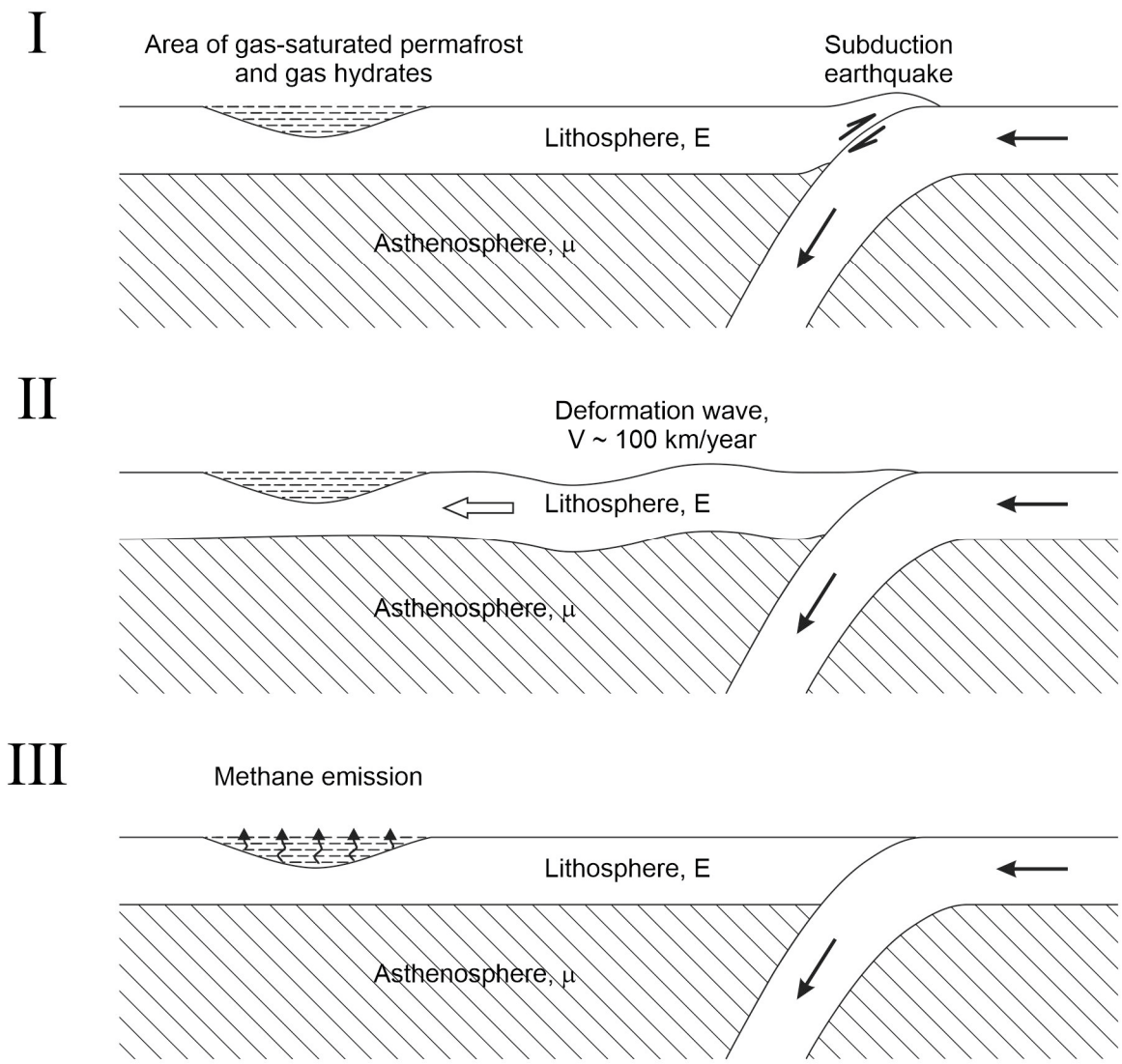

Figure 3. Scheme of the seismogenic trigger mechanism of methane emission on the polar shelf due to the destructive effect on gas hydrates of deformation waves caused by strong earthquakes in the subduction zone. (**I**): Large-magnitude earthquake generating the tectonic wave, (**II**): Propagation of the tectonic wave, (**III**): Methane emission caused by the tectonic wave-associated stresses arriving in methane-saturated and hydrate-bearing permafrost area.

Due to the rather large distance between the Arctic Shelf and the Aleutian subduction zone (about 2000 km), the question arises about the degree of attenuation of deformation waves that have reached the shelf and the magnitude of the corresponding additional stresses acting in the gas hydrate region. As calculations show, in the original Elsasser model [32], a strong attenuation of the amplitude of deformation waves and the stresses carried by them occurs at distances of about 200–300 km from the source of the disturbance generation. A similar attenuation of deformation disturbances in the lithosphere was obtained in subsequent works generalizing the Elsasser model, within the framework of a purely mechanical approach [33–39]. Hence, it follows that in the case of a purely mechanical approach, tectonic deformation disturbances in the lithosphere at considerable distances of about 2000 km from the source of generation will be too small to cause any trigger effects. However, this conclusion loses its force if we consider the thermomechanical model of deformation waves, which takes into account the phase transition at the boundary between the lithosphere and the asthenosphere, leading to partial melting of the substance of the lithosphere or, conversely, the crystallization of the substance of the asthenosphere [42,43].

Calculations show that with such a more realistic approach, the attenuation of deformation waves, becomes much weaker, and they are able to transfer significant additional stresses (of the order of 0.1 MPa) over distances of more than 1000 km [43]. The specified thermomechanical model of deformation waves is suitable for use as a trigger mechanism for the destruction of metastable gas hydrates since it provides a long-range transfer of sufficiently noticeable additional stresses for several thousand km.

A specific description of the trigger mechanism of zonal destruction of the microstructure of permafrost gas-saturated rocks containing ice and metastable gas hydrates under the influence of a slight change in external pressure was given in the works [15,18]. Thus, it was shown that small regional changes in the stress–strain state of the lithosphere, including frozen rocks of the sedimentary layer, can cause the release of sufficiently large volumes of gas trapped in them, its filtration through a medium with double porosity (bearing rock with inclusions) [16,18] and subsequent emissions into the water column and atmosphere.

This is ultimately the proposed physical mechanism of a sharp activation of methane emissions and climate warming in the Arctic as a result of a strong mechanical disturbance of the marginal region of the Arctic lithosphere caused by the large earthquakes in the Aleutian subduction zone, the transmission of this disturbance by tectonic deformation waves to the Arctic shelf and adjacent land, as well as the trigger effect of the release of methane from permafrost rocks and metastable gas hydrates.

3. Correlation between Seismogenic Tectonic Waves and Glacier Destruction in Antarctica

Turning to the question of applying the concept of tectonic wave deformation discussed above to the analysis of modern processes occurring in the south polar region of the Earth, we note that Antarctica is surrounded by the South Pacific Ocean, Chilean, and Tonga–Kermadec–Macquarie subduction zones, in which large earthquakes occur from time to time. These earthquakes, as well as in the case of the Aleutian subduction zone, should generate tectonic deformation waves that propagate in different directions, including in the direction of Antarctica, with speeds of about 100 km/year. By analogy with the Arctic, it can be assumed that these waves, using trigger mechanisms, will trigger the destruction of various natural objects in a metastable state, primarily glaciers and gas hydrates located under them, leading to methane emissions and climate warming.

To substantiate the hypothesis put forward, let us consider the spatial–temporal correlation between the large earthquakes that occurred in the South Pacific subduction zones and the phases of the destruction of the glaciers of the Antarctic Peninsula in West Antarctica. Figure 4 shows a map of the heights of the surface of the Antarctic Peninsula, on which today's largest ice shelves are marked in blue: Larsen (32,000 km^2), George VI (24,000 km^2), and Wilkins (10,000 km^2), the white color shows the sea without ice shelf.

Figure 5 shows the areas of the large earthquakes that occurred in the time intervals of 1960–2000 (Figure 5a) and 2001–2022 (Figure 5b) in the lithosphere of the South Pacific Ocean surrounding Antarctica, the Chilean, and Tonga–Kermadec–Macquarie subduction zones. The modern chronology of glacier destruction begins with the northern block A of the Larsen Glacier (Figure 4), which was destroyed in 1995. The subduction zone closest to the Antarctic Peninsula, generating the large earthquakes, is the Chilean zone, where in 1960 the most powerful mega-earthquake (in the history of instrumental observations) occurred, with a maximum magnitude of M = 9.6 (Figure 5a).

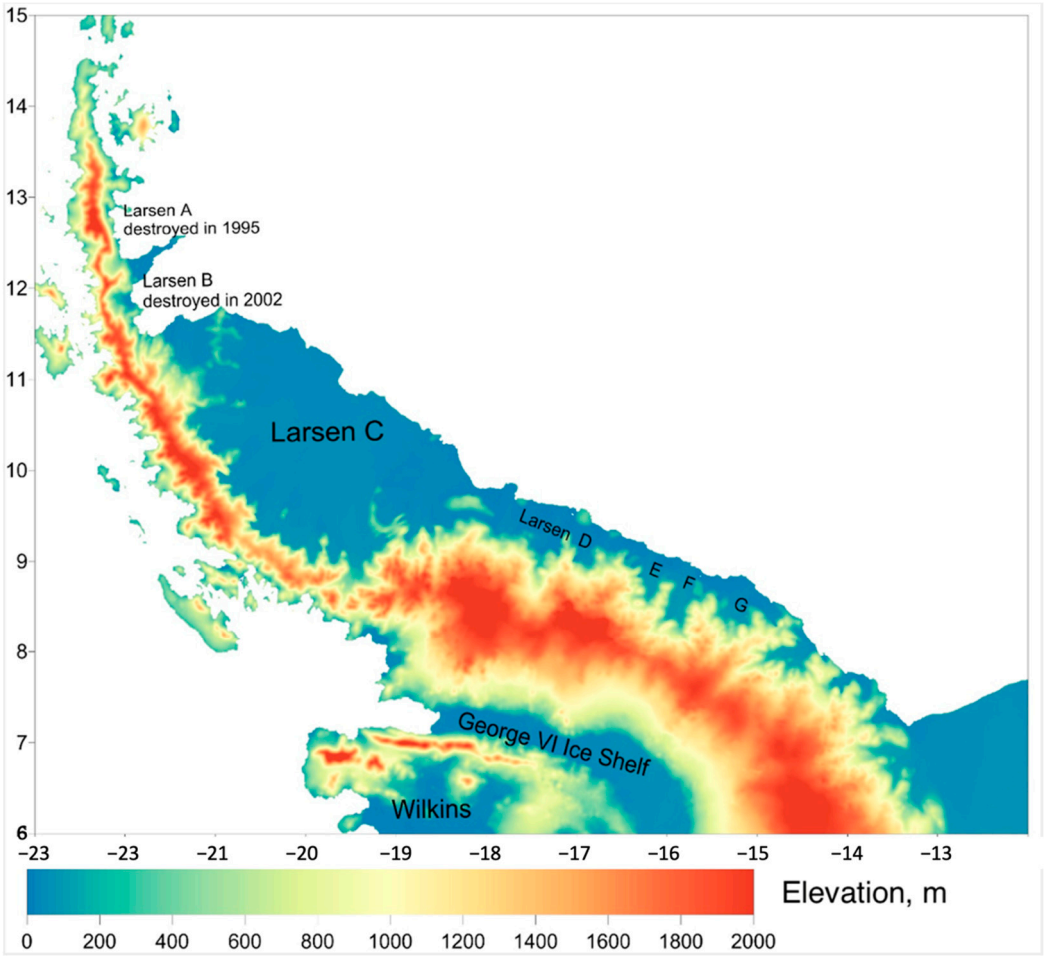

Figure 4. Surface topography map for Antarctic Peninsula.

In the same year, 1960, approximately in the same part of the subduction zone, two more large earthquakes occurred, at M = 8.6 and 8.3 (Figure 5a).

Based on the seismogenic trigger mechanism, it can be assumed that tectonic deformation waves caused by these events, propagating at a speed of about 100 km/year, reaching the Antarctic Peninsula, led to the destruction of the northern block A of the Larsen Glacier (Figure 4), which occurred in 1995, i.e., 35 years after the large earthquakes of 1960 (Figure 5a). This time lag corresponds to a distance of about 3300 km between the earthquake foci and the northern tip of the Antarctic Peninsula, which is traversed by a tectonic wave at a speed of about 100 km/year. The destruction of the Wilkins Glacier in 1998 may also be related to tectonic waves from the 1960 earthquakes in Chile. The delay of three years compared to the destruction of the Larsen A Glacier may be due to the fact that the Wilkins Glacier lies southwest of the Larsen A Glacier and therefore the tectonic wave came later (Figure 4). It should be noted that a slightly smaller time shift for the Arctic, which was estimated at 20 years [10], is presumably associated with a smaller distance from the foci of the large earthquakes in the Aleutian subduction zone to the Arctic Shelf (about 2000 km) compared with the distance from the foci of Chilean earthquakes to the Larsen Glacier in Antarctica. It is possible that the formation of faults in the George VI glacier in 2001 is also associated with the set of tectonic waves that came from the large earthquakes of 1960.

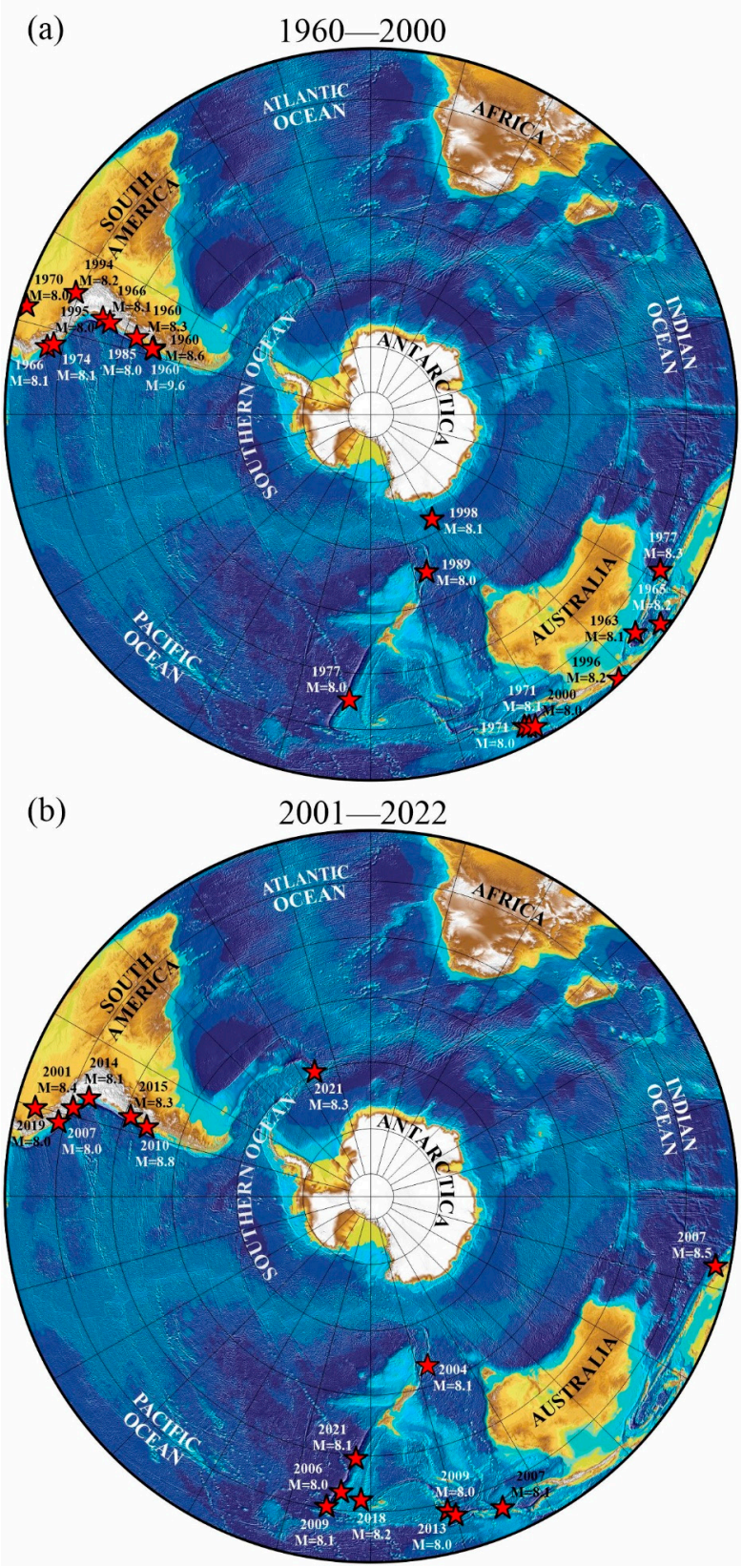

Figure 5. Sources of the large earthquakes in the Chilean and Kermadec–Macquarie subduction zones in the second half of the 20th century and the beginning of the XXI century. Red stars correspond to focal zones. (**a**) During 1960–2000, (**b**) During 2001–2022.

The next collapse of the Larsen Glacier took place in 2002 in segment B, adjacent to Block A from the south (Figure 4) [44]. If we assume that the time shift between the source of the tectonic deformation wave excitation and its arrival in the glacier destruction zone, as in the previous case, is approximately 35 years, then such a potential source exists in the Chilean subduction zone; this is the large earthquake with a magnitude of M = 8.1 that occurred here in 1966 (Figure 5a). It is possible that the same earthquake led to the repeated collapse of the Wilkins Glacier in 2008–2009 southwest of the Larsen B Glacier due to the set of tectonic wave arrivals. In particular, the ice bridge connecting part of the ice shelf with Charcot Island collapsed.

In 2010, a large iceberg broke off from the George VI Glacier. The delay in the destruction of the George VI Glacier relative to the destruction of its neighbor Wilkins Glacier can be explained by its greater stability due to being in a narrow strait. In the future, the Larsen B glacier underwent another phase of destruction in 2022.

The Larsen C ice shelf experienced an unusual surge in ambient temperature rise and surface melting at the end of summer 2015. In 2017, a huge iceberg broke off from this glacier [45]. These events can be associated with the large earthquake with a magnitude of M = 8.0 that occurred in the Chilean subduction zone in 1985 (Figure 5a) (again, a time shift of 30–35 years is obtained). A little earlier in 2013, another phase of collapse of the Wilkins Glacier, already significantly broken by the previous series of tectonic waves, occurred. Note that after 2013, the collapse of the Wilkins Glacier was no longer observed.

It is interesting to compare and analyze from the standpoint of the seismogenic trigger hypothesis some anomalous geophysical and climatic phenomena observed in the Antarctic Peninsula area quite recently, in 2020 and 2021. First of all, we note the seismic activity that unexpectedly appeared in the second half of 2020 in the form of a large swarm of earthquakes of small magnitude in the amount of more than 80 thousand events that occurred near the tip of the Antarctic Peninsula [46]. This phenomenon was proposed to be explained by the "awakening" of a long-dormant underwater volcano located under the seabed in the Bransfield Strait between the South Shetland Islands and the northwestern tip of Antarctica. This area is associated with the subduction zone of the Phoenix Plate, sinking under the edge of Antarctica, which is a continuation to the south of the large-scale Chilean subduction zone of the Pacific Plate.

The alternative point of view proposed by us is that the occurrence of a swarm of small-magnitude earthquakes is due to additional stresses in the lithosphere "brought" by a tectonic wave to this area in 2020, caused by the large earthquake with a magnitude of 8.0 that occurred in the Chilean subduction zone in 1985 (Figure 5a) (a time shift of 35 years). However, even if we accept the hypothesis of the volcano's awakening, it is logical to associate the specific time of this awakening with the arrival of a tectonic deformation wave at this place, which was a mechanical trigger for the beginning of magma movement along the opening cracks, which could cause the observed swarm of earthquakes. In 2022, the same tectonic deformation wave led to the collapse of the remaining part of the Larsen B ice shelf on the northeastern edge of the Antarctic Peninsula.

Based on the general concept of the seismogenic trigger mechanism, it is interesting to trace the relationship between the large earthquakes in the southernmost segment of the subduction zone of the southwestern part of the Pacific Plate and the destruction of the Ross Ice Shelf closest to this segment (Figure 5a). In 2000, the largest iceberg in the entire history of observations broke away from it. Within the framework of the seismogenic trigger approach, this event can be associated with the large earthquake with a magnitude of M = 8.0 that occurred in 1989 south of New Zealand near Macquarie Island (distance ~3100 km, M = 8.0) (Figure 5a). A shorter delay time (11 years) is associated with the arrival of a tectonic wave compared to geodynamic systems "Aleutian Arc-Arctic Shelf" (about 20 years) or "Chilean subduction zone-Antarctic Peninsula" (30–35 years) in the framework of the model under consideration [43] is due to the difference in the rheological parameters of the lithosphere and asthenosphere in different regions that determine the

speed of propagation of tectonic deformation waves, in particular, the relatively lower viscosity of the asthenosphere in the area between New Zealand and Antarctica.

In recent decades, several major earthquakes have occurred in the southern part of the Chilean subduction zone (1995, 2001, 2007, 2010, 2014, and 2015) (Figure 5a,b), and in 2021 there was a large earthquake in the Sandwich Trench (Figure 5b). The arrival of tectonic deformation waves from these earthquakes, according to the presented concept, will lead to further collapse of the Larsen, Wilkins, George VI glaciers, and other shelf glaciers of the Antarctic Peninsula in the near future.

4. Trigger Mechanisms for Accelerating the Movement of Glaciers, Their Destruction, and Methane Emissions from Subglacial Gas Hydrates

The ice of Antarctica consists of covered glaciers (lying on the bedrock), shelf glaciers, and sea ice. The thickness of the changing sea ice is several meters, the shelf glaciers range from tens of meters near the coast to a kilometer in the rear, while the thickness of the cover glaciers in some areas of Antarctica exceeds 4 km (Figure 6). Ice thickness map was compiled using the dataset from https://secure.antarctica.ac.uk/data/bedmap2/, accessed on 20 August 2022 [47].

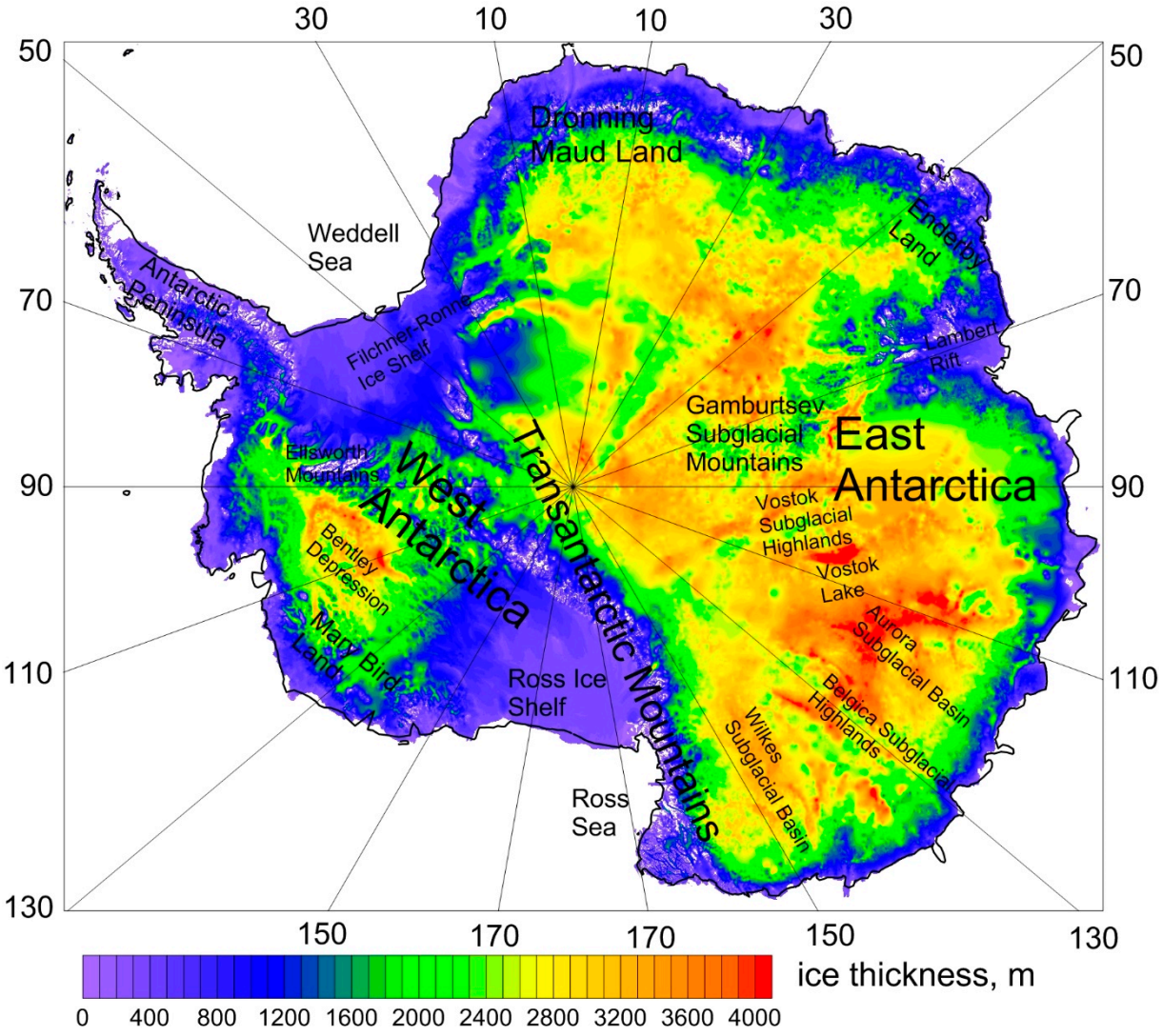

Figure 6. Ice thickness map of Antarctica based on Bedmap2 dataset [47].

A shelf glacier is an ice mass floating in the ocean, attached to the frontal part of a covered glacier sliding along the bedrock into the ocean (Figure 7). Covered glaciers lie on

the sedimentary, crystalline, or metamorphic rocks, and often the subglacial surface lies below sea level. At the same time, near the coast glaciers lie mainly on sedimentary rocks. Shelf glaciers in a stable situation can prevent the covered glaciers located behind them from sliding into the sea. In turn, sea ice surrounding ice shelves affects the stability of ice shelves, protecting them from the effects of ocean waves and storms [48].

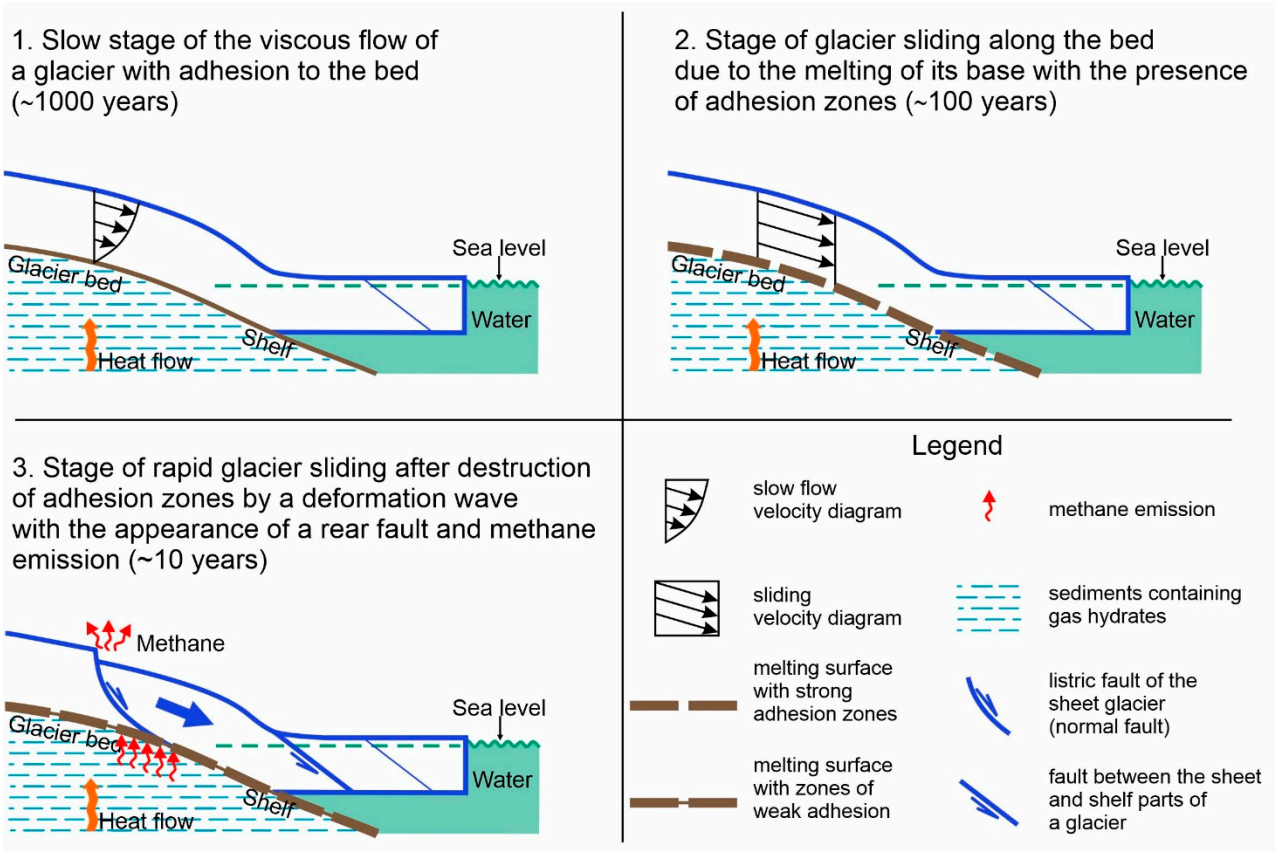

Figure 7. Scheme of various stages and regimes of ice shelf movement for the area of the Antarctic Peninsula.

Figure 7 shows a simplified diagram of the various modes of movement of the cover-shelf glacier, reflecting the different stages of its thermomechanical evolution. The first initial stage of evolution corresponds to the slow sliding of the covered glacier along the bedrock under conditions of complete adhesion of the glacier sole with the surface of the underlying sedimentary rocks. The flow of a glacier is similar to the runoff of a very viscous liquid from an inclined bed in conditions of its adhesion to a fixed base. The speed of movement of the glacier surface depends on a number of different conditions (glacier feeding regime, geometry of the bedrock, ambient temperature, adhesion to the rocks of the base, etc.) and can vary widely, from the first meters to hundreds of meters per year. For example, during the first "cold" stage of the slow flow of the glacier in conditions of its complete adhesion to the bedrock, the total displacement of the glacier over a thousand years may be only a few km (Figure 7).

The second "warm" stage of glacier movement in our scheme (Figure 7) is fundamentally different in that ice melting zones appear on the bottom of the glacier as a result of the prolonged action of increased heat flow coming from beneath, which is typical for significant areas of West Antarctica [49,50] (Figure 8).

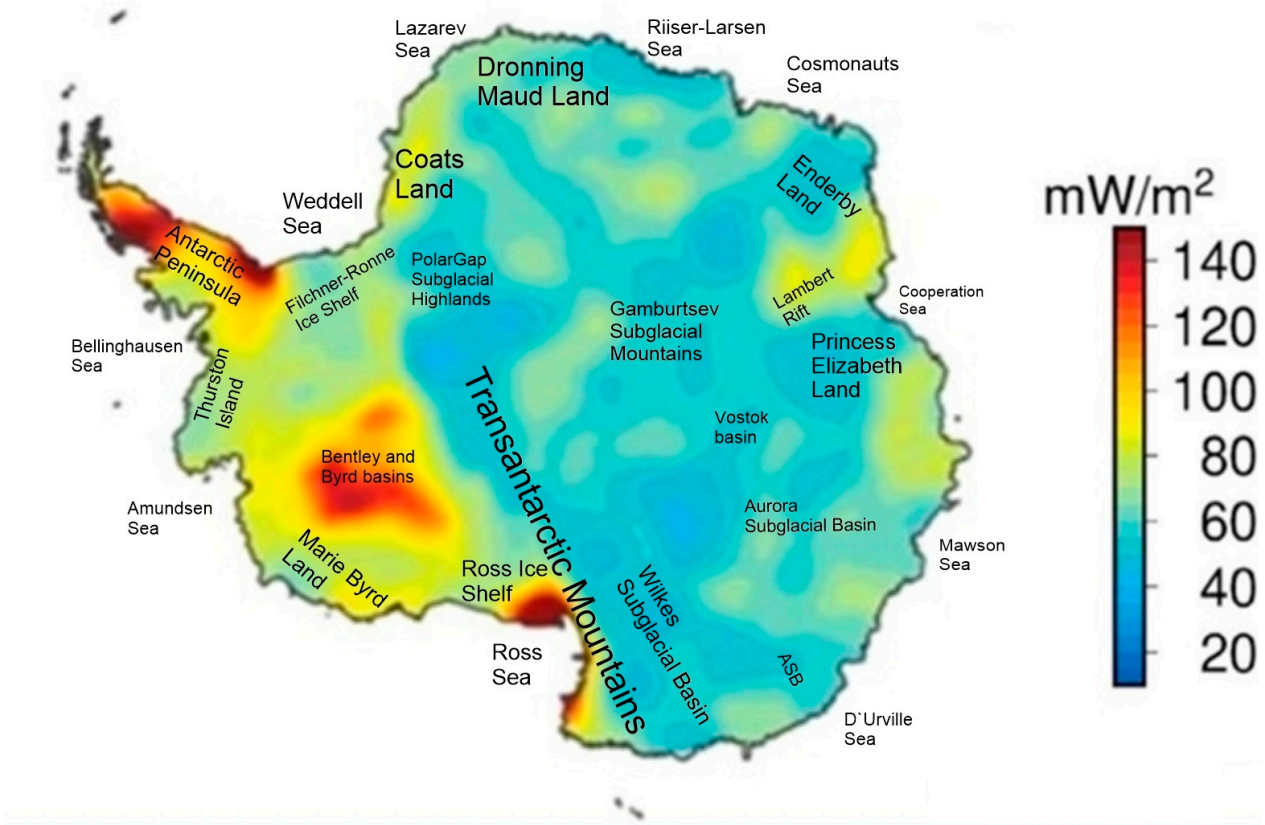

Figure 8. Heat flux map of Antarctica, modified after [50].

When a water layer of lubricant appears on the sole of the glacier, the mode of its movement changes significantly, since (in the zones of ice melting) the ice mass begins to slip almost without friction along the bedrock surface [51]. Rapid catastrophic sliding of the glacier as a whole does not occur at this stage due to the fact that melting on its sole occurs spatially unevenly (due to the uneven geometry of the base, variations in pressure on the sole of the glacier varying in thickness and other physical and mechanical reasons) and "dry" areas remain between the melting zones in which adhesion is maintained of a glacier with a bedrock surface. The second stage of the evolution of a glacier with a partially melted sole is preparatory to the third stage and can last for several decades until the dry zones in the contact zone of interaction between the glacier and the bedrock disappear. It should be noted that the idea of the existence of local areas of adhesion on the contact surface of the displacement of adjacent crustal blocks is widely used in the analysis of the development of the large earthquake source in the contact area of interaction of lithospheric plates in subduction zones, called "asperity"-the roughness of the contact surface [52].

The third catastrophic stage of glacier movement is characterized by the disappearance of adhesion zones (roughness) on the contact surface of the glacier's interaction with the underlying bed and the breakdown of the glacier from the bedrock, accompanied by the destruction of its rear sections with the appearance of faults and cracks (Figure 7). In our concept, the third stage of glacier disruption and block movement occurs as a result of the arrival of tectonic deformation waves in Antarctica from the surrounding sources of the large subduction earthquakes and the destruction of the remaining adhesion zones (roughness) on the contact surface due to additional stresses brought by the tectonic deformation wave. This is the seismogenic trigger mechanism of glacier collapse, which takes place when the third catastrophic stage of glacier movement occurs. The rapid block sliding of the glacier, along with the destruction of the rear region of the covered glacier, occur under stretching conditions in the form of concave faults. Destruction also occurs in the junction zone of the frontal part of the covered glacier with a floating ice shelf

(Figure 7). Such collapse occurs under conditions of compression and partial displacement of the frontal part of the covered glacier under the edge of the shelf glacier with the formation of an inclined fault in the junction zone by analogy with the initial stage of the plate subduction process under the island arc or the edge of the continent (Figure 7). The rapid block movement of the glacier at the third stage of evolution stops as a result of the action of two main factors: firstly, the covered glacier rapidly sliding into the ocean experiences a blocking effect from the adjacent part of the shelf glacier and, secondly, the fractured material in the destruction zone experiences convective air cooling which causes the freezing, and, as a result, a new zone of adhesion of the glacier appears, which can stop its movement. However, the movement of the glacier may resume again if a new tectonic deformation wave "cuts off" the adhesion zone that has arisen as a result of freezing. Such repeated rapid movements of glaciers, as shown above, were observed during the collapse of glaciers of the Antarctic Peninsula.

The destruction of the junction zone of the cover and shelf glaciers with the formation of an inclined discontinuous surface of the thrust will be accompanied by a sufficiently strong ice quake (by analogy with a large earthquake in the lithosphere subduction zone) and the occurrence of seismic elastic waves in the body of the shelf glacier. The resulting waves, passing through the fractured weakened zones of the ice shelf, located at a sufficiently large distance from the place of its junction with the covered glacier, will lead to repeated destruction of these remote weakened zones of the glacier. In this way, the destruction of peripheral sections of ice shelves (for example, the Larsen C glacier) can be explained as a sequential effect of the trigger action of tectonic deformation waves in the lithosphere and seismic waves in the body of the glacier itself.

The third stage of the movement and destruction of the glacier in the concept under consideration is directly related to the rapid warming of the climate in Antarctica. To clarify this issue, let us turn to the structure of the Antarctic crust, which is characterized by the presence of extensive sedimentary basins that arose during its geological evolution [53,54] (Figure 9).

For example, the crust of West Antarctica was subjected to rift stretching during its evolution, which led to the formation of sedimentary basins, underlaying, in particular, the seas surrounding West Antarctica [53–58] (Figure 9). Seismic data and offshore drilling data show that the upper layer of the sediments here is represented by Cenozoic molasses with permafrost rocks. Above these rocks, there is a shallow sea and ice shelves. According to modern concepts [59,60], the sedimentary rocks underlying the ice of Antarctica may contain large reserves of methane in the form of gas hydrates. The estimates made of these reserves [61] are comparable to estimates of reserves of methane hydrates contained in vast areas of permafrost in the Arctic region. Therefore, as in the Arctic, the release of methane from gas hydrates in sedimentary rocks during the destruction of the ice cover can lead to its emission into the atmosphere and climate warming. In this regard, the recent detection of methane emissions at the bottom of the Ross Sea in the area of the existence of gas hydrates in the sedimentary column is of great interest [61].

A possible mechanism for the collapse of Antarctic glaciers, leading to methane emissions, is shown in Figure 7. As noted above, in the rear zone of faults and cracks of a rapidly sliding glacier, hydrostatic pressure falls on the underlying layers of sediments, presumably containing gas hydrates. This will lead to a violation of the metastable state of gas hydrates and, as a consequence, to the release of methane trapped in micropores of low-permeable frozen rocks and partially dissociated metastable gas hydrate particles surrounded by thin layers of ice (Figure 1). The free methane extracted from gas hydrates will be able to quickly filter through the fractured medium of a partially destroyed glacier and be released into the atmosphere [15–18]. This is the proposed physical mechanism of the sharp activation of methane emissions and climate warming in West Antarctica as a result of the destruction of glaciers by tectonic deformation waves caused by the large earthquakes in the Chilean and Kermadec–Macquarie subduction zones closest to Antarctica, as well

as the trigger effect of the release of methane from permafrost sedimentary rocks and metastable gas hydrates.

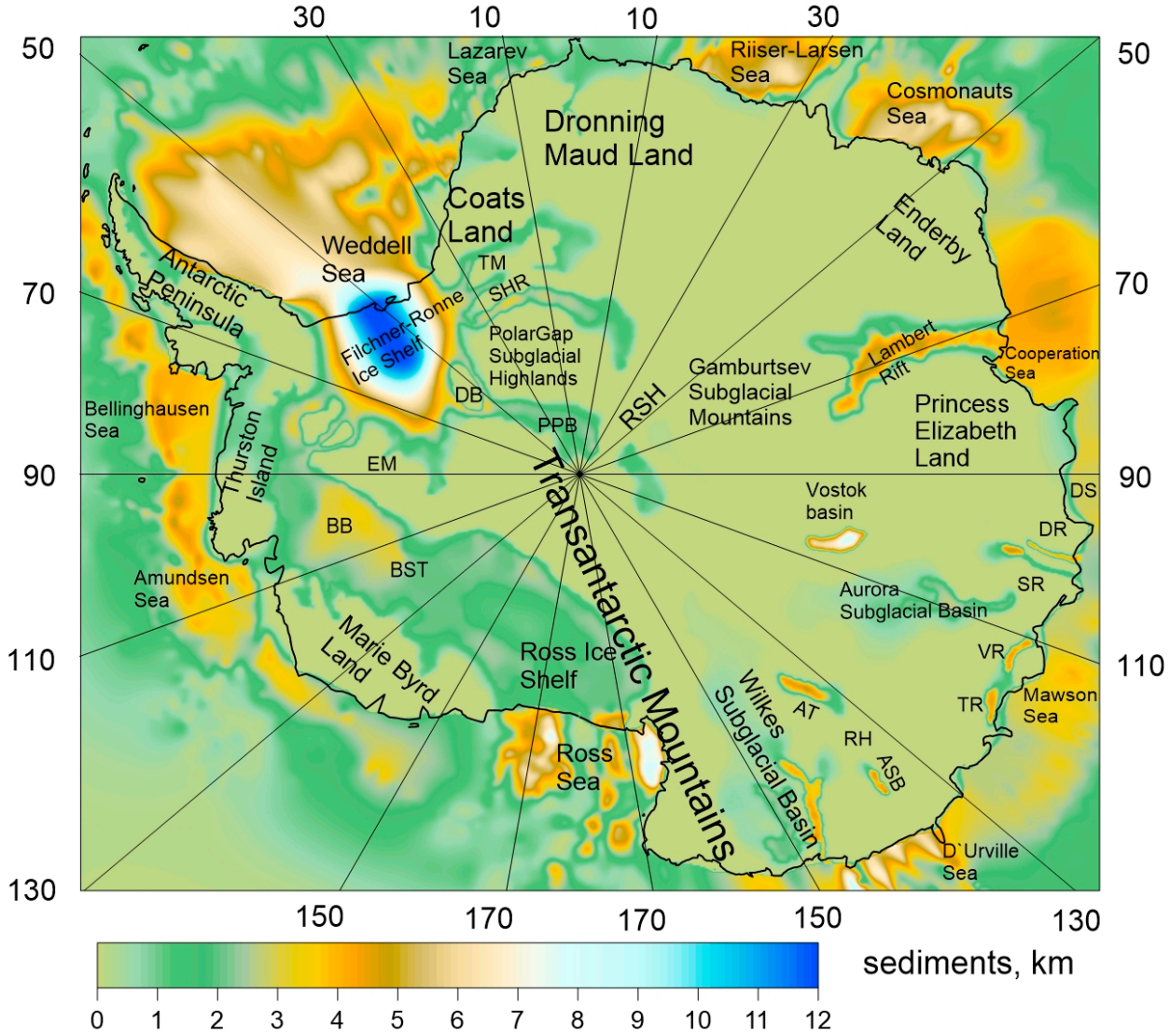

Figure 9. Sediment thickness map for South Pole area [54].

5. Conclusions

In the Arctic, the trigger activation of methane emissions began in the late 1970s of the previous century, when tectonic waves caused by large earthquakes in the Aleutian arc in 1957–1965 came to the Arctic shelf, having traveled a distance of about 2000 km at a speed of about 100 km/year for about 20 years. This process was associated with the sharp warming of the environment in the Arctic in 1979–1980 due to the greenhouse effect of methane emissions.

In Antarctica, the modern glacier collapse began at the end of the last century (and continues to date), mainly occurring in its western part, primarily the Antarctic Peninsula. The trigger mechanism of glacier collapse is associated with tectonic deformation waves caused by large earthquakes in the subduction zones surrounding Antarctica. Thus, the collapse of the Larsen A Glacier in 1995 and that of the Wilkins Glacier in 1998 are associated with tectonic waves from the great earthquake of 1960, M = 9.6 in the Chilean subduction zone. The collapse of the Larsen B glacier in 2002 and the repeated large collapse of the Wilkins Glacier in 2008–2009 southwest of the Larsen B Glacier probably occurred as a result of the arrival of tectonic waves from another large earthquake in 1966, M = 8.1. The

breakaway of the giant iceberg A-68 from the Larsen C ice shelf in 2017 can be associated with the 1985 M = 8.0 earthquake.

The proposed seismogenic trigger mechanism for accelerating the movement of glaciers and the release of methane from metastable gas hydrates due to the arrival of tectonic deformation waves from the sources of the large subduction earthquakes in the South Pacific Ocean makes it possible to explain the climate warming and the ice shelves collapse in West Antarctica that began at the end of the 20th century and is currently continuing.

The mechanism of glacier collapse and climate warming in Antarctica considered in this paper does not negate the existing ideas about the influence of warm sea currents and atmospheric flows on these processes [62]. The proposed approach expands these ideas by including in the general analysis a geodynamic factor aimed at explaining the reason for the beginning of a sharp intensification of glacier collapse and climate warming in West Antarctica since the end of the last century and the intensification of these processes in the current century. The proposed mechanism also makes it possible to explain why the polar regions are heating up significantly faster than the main part of our planet, linking this fact with large emissions of greenhouse methane into the atmosphere in the polar regions. It should be noted that this geodynamic model predicts a further acceleration of the glacier collapse and climate warming in Antarctica in the near future due to an unprecedented increase in the frequency of large earthquakes in the South Pacific in the late 20th and early 21st centuries.

Author Contributions: Conceptualization, L.I.L. and A.A.B.; methodology, A.A.B., I.S.V. and Y.V.G.; software, A.A.B., I.S.V. and Y.V.G.; validation, A.A.B., I.S.V. and Y.V.G.; formal analysis, A.A.B., I.S.V., Y.V.G. and L.I.L. investigation, M.M.R., A.A.B., I.S.V., Y.V.G. and L.I.L.; resources, L.I.L. and I.P.S.; data curation, A.A.B., I.S.V., Y.V.G. and D.A.A.; writing—original draft preparation, A.A.B. and L.I.L.; writing—review and editing, all authors; visualization, A.A.B., I.S.V., Y.V.G. and D.A.A.; supervision, L.I.L.; project administration, L.I.L. and I.P.S.; funding acquisition, I.P.S. All authors have read and agreed to the published version of the manuscript.

Funding: This study was supported by Tomsk State University under the program *Prioritet 2030* run by the Ministry of Science and Education of the Russian Federation (conceptualization, problem statement), with partial support from the Russian Science Foundation, grant no. 22-67-00025 (investigation, formal analysis) and the State Assignment of the Institute of Earthquake Prediction Theory and Mathematical Geophysics RAS No. AAAA-A19-119011490131-3 (data acquisition and validation).

Data Availability Statement: Not applicable.

Acknowledgments: We thank the Editor and anonymous reviewers for constructive comments which helped to improve the manuscript.

Conflicts of Interest: The authors declare no conflict of interest.

References

1. Yakushev, V.S. *Natural Gas and Gas Hydrates in Cryolithozone*; VNIIGAZ: Moscow, Russia, 2009; 192p. (In Russian)
2. Yakushev, V.S.; Istomin, V.A. Gas hydrates self-preservation effect. In *Physics and Chemistry of Ice*; Maeno, N., Hondoh, T., Eds.; Hokkaido University Press: Sapporo, Japan, 1992; pp. 136–140.
3. Yakushev, V.S.; Chuvilin, E.M. Natural gas and hydrate accumulation within permafrost in Russia. *Cold Reg. Sci. Technol.* **2000**, *149*, 46–50. [CrossRef]
4. Chuvilin, E.M.; Guryeva, O.M. Experimental study of self-preservation effect of gas hydrates in frozen sediments. In Proceedings of the 9th International Conference on Permafrost, Fairbanks, Alaska, 23 June–3 July 2008; pp. 263–267.
5. Chuvilin, E.; Bukhanov, B.; Davletshina, D.; Grebenkin, S.; Istomin, V. Dissociation and self-preservation of gas hydrates in permafrost. *Geosciences* **2018**, *8*, 431. [CrossRef]
6. Takeya, S.; Ebinuma, T.; Uchida, T.; Nagao, J.; Narita, H. Self-preservation effect and dissociation rates of CH_4 hydrate. *J. Cryst. Growth* **2002**, *237–239*, 379–382. [CrossRef]
7. Stern, L.A.; Circone, S.; Kirby, S.H.; Durham, W.B. New insights into phenomenon of anomalous or «self» preservation of gas hydrates. In Proceedings of the Fourth Intrernational Conference on Gas Hydrates, Yokohama, Japan, 19–23 May 2002; Volume 1, pp. 673–677.
8. Istomin, V.A.; Yakushev, V.S.; Makhonina, N.A.; Kwon, V.G.; Chuvilin, E.M. Self-preservation effect in gas hydrates. *Gas Industr.* **2006**, *4*, 36–46. (In Russian)

9. Davidson, D.A.; Garg, S.K.; Gough, S.R.; Handa, Y.P.; Ratcliffe, C.I.; Ripmeester, J.A.; Tse, J.S.; Lawson, W.F. Laboratory analysis of naturally occurring gas hydrate from sediment of the Gulf Mexico. *Geochim. Et Cosmochim. Acta* **1986**, *50*, 619–623. [CrossRef]
10. Lobkovsky, L.I. Seismogenic-triggering mechanism of gas emission activizations on the Arctic shelf and associated phases of abrupt warming. *Geosciences* **2020**, *10*, 428. [CrossRef]
11. Makogon, Y.F. *Natural Gas Hydrates*; Nedra: Moscow, Russia, 1974; 208p. (In Russian)
12. Cherskiy, N.V.; Tsarev, V.P.; Nikitin, S.P. *Study and Prediction of the Conditions of Gas Accumulations in Hydrate Deposits*; Siberian Branch of Academy of Sciences of the USSR: Yakutsk, Russia, 1983; 156p. (In Russian)
13. Chuvilin, E.M.; Perlova, E.F. Forms of occurrence and conditions of formation of the gaseous component of permafrost rocks. *Bull. Mosc. Univ. Bull. Ser. Geol.* **1999**, *5*, 57–59.
14. Dillon, W.; Max, V. Oceanic gas hydrates. In *Natural Gas Hydrate in Oceanic and Permafrost Environment*; Kluwer, M., Ed.; Academic Publishers: Cambridge, MA, USA, 2000; pp. 61–76.
15. Barenblatt, G.I.; Lobkovsky, L.I.; Nigmatulin, R.I. A mathematical model of gas outflow from gas-saturated ice and gas hydrates. *Dokl. Earth Sci.* **2016**, *470*, 1046–1049. [CrossRef]
16. Lobkovsky, L.I.; Ramazanov, M.M. Theory of filtration in a double porosity medium. *Dokl. Earth Sci.* **2019**, *484*, 105–108. [CrossRef]
17. Lobkovsky, L.I.; Ramazanov, M.M. A generalized model of filtration in a fractured-porous medium with low-permeable inclusions and its possible applications. *Izvestiya Phys. Solid Earth* **2022**, *58*, 281–290. [CrossRef]
18. Lobkovsky, L.I.; Ramazanov, M.M.; Semiletov, I.P.; Alekseev, D.A. Mathematical model of the decomposition of unstable gas hydrate accumulations in the cryolithozone. *Geosciences* **2022**, *12*, 345. [CrossRef]
19. Bykov, V.G. Prediction and observation of strain waves in the Earth. *Geodyn. Tectonophys.* **2018**, *9*, 721–754. (In Russian) [CrossRef]
20. Mogi, K. Migration of seismic activity. *Bull. Earthq. Res. Inst.* **1968**, *46*, 53–74.
21. Kasahara, K. Migration of crustal deformation. *Tectonophysics* **1979**, *13*, 329–341. [CrossRef]
22. Di Giovambattista, R.; Tyupkin, Y. Cyclic migration of weak earthquakes between Lunigiana earthquake of October 10, 1995 and Reggio Emilia earthquake of October 15, 1996 (Northern Italy). *J. Seismol.* **2001**, *5*, 147–156. [CrossRef]
23. Molchanov, O.A.; Uyeda, S. Upward migration of earthquake hypocenters in Japan, Kurile–Kamchatka and Sunda subduction zones. *Phys. Chem. Earth* **2009**, *34*, 423–430. [CrossRef]
24. Liu, M.; Stein, S.; Wang, H. 2000 years of migrating earthquakes in North China: How earthquakes in midcontinents differ from those at plate boundaries. *Lithosphere* **2011**, *3*, 128–132. [CrossRef]
25. Trofimenko, S.V.; Bykov, V.G.; Merkulova, T.V. Space-time model for migration of weak earthquakes along the northern boundary of the Amurian microplate. *J. Seismol.* **2017**, *21*, 277–286. [CrossRef]
26. Zalohar, J. The Omega-Theory: A New Physics of Earthquakes. In *Developments in Structural Geology and Tectonics*, 1st ed.; Elsevier: Amsterdam, The Netherlands, 2018; Volume 2, 558p.
27. Kuzmin, Y.O. Deformation autowaves in fault zones. *Izvestiya Phys. Solid Earth* **2012**, *48*, 1–16. [CrossRef]
28. Reuveni, Y.; Kedar, S.; Moore, A.; Webb, F. Analyzing slip events along the Cascadia margin using an improved subdaily GPS analysis strategy. *Geophys. J. Int.* **2014**, *198*, 1269–1278. [CrossRef]
29. Harada, M.; Furuzawa, T.; Teraishi, M.; Ohya, F. Temporal and spatial correlations of the strain field in tectonic active region, southern Kyusyu, Japan. *J. Geodyn.* **2003**, *35*, 471–481. [CrossRef]
30. Bella, F.; Biagi, P.F.; Caputo, M.; Della Monica, G.; Ermini, A.; Manjgaladze, P.; Sgrigna, V.; Zilpimian, D. Very slow-moving crustal strain disturbances. *Tectonophysics* **1990**, *179*, 131–139. [CrossRef]
31. Yoshioka, S.; Matsuoka, Y.; Ide, S. Spatiotemporal slip distributions of three long-term slow slip events beneath the Bungo Channel, southwest Japan, inferred from inversion analyses of GPS data. *Geophys. J. Int.* **2015**, *201*, 1437–1455. [CrossRef]
32. Elsasser, W.V. Convection and stress propagation in the upper mantle. In *The Application of Modern Physics to the Earth and Planetary Interiors*; Runcorn, S.K., Ed.; John Wiley: New York, NY, USA, 1967; pp. 223–246.
33. Melosh, H.J. Nonlinear stress propagation in the Earth's upper mantle. *J. Geophys. Res.* **1976**, *32*, 5621–5632. [CrossRef]
34. Bott, M.H.P.; Dean, D.S. Stress diffusion from plate boundaries. *Nature* **1973**, *243*, 339–341. [CrossRef]
35. Anderson, D.L. Accelerated plate tectonics. *Science* **1975**, *187*, 1077–1079. [CrossRef]
36. Savage, J.C. A theory of creep waves propagating along a transform fault. *J. Geophys. Res.* **1971**, *76*, 1954–1966. [CrossRef]
37. Ida, Y. Slow-moving deformation pulses along tectonic faults. *Phys. Earth Planet. Int.* **1974**, *9*, 328–337. [CrossRef]
38. Rice, J.R. The mechanics of earthquake rupture. In *Physics of the Earth's Interior*; Dziewonski, A.M., Boschi, E., Eds.; Italian Physical Society: Amsterdam, The Netherlands, 1980; pp. 555–649.
39. Ricard, Y.; Husson, L. Propagation of tectonic waves. *Geophys. Res. Lett.* **2005**, *32*, L17308. [CrossRef]
40. Shakhova, N.; Semiletov, I.; Sergienko, V.; Lobkovsky, L.; Yusupov, V.; Salyuk, A.; Salomatin, A.; Chernykh, D.; Kosmach, D.; Panteleev, G.; et al. The East Siberian Arctic Shelf: Towards further assessment of permafrost-related methane flux and role of sea ice. *Phil. Trans. R. Soc. A* **2015**, *373*, 20140451. [CrossRef]
41. Shakhova, N.; Semiletov, I.; Gustafsson, O.; Sergienko, V.; Lobkovsky, L.; Dudarev, O.; Tumskoy, V.; Grigoriev, M.; Mazurov, A.; Salyuk, K.; et al. Current rates and mechanisms of subsea permafrost degradation in the East Siberian Arctic Shelf. *Nat. Comm.* **2017**, *8*, 15872. [CrossRef] [PubMed]
42. Garagash, I.A.; Lobkovsky, L.I. Deformation tectonic waves as a possible trigger mechanism for the activation of methane emissions in the Arctic. *Arct. Ecol. Econ.* **2021**, *11*, 42–50. (In Russian) [CrossRef]

43. Lobkovsky, L.I.; Ramazanov, M.M. Thermomechanical waves in the elastic lithosphere–viscous asthenosphere system. *Fluid Dyn.* **2021**, *56*, 765–779. [CrossRef]
44. Scambos, T.A.; Bohlander, J.A.; Shuman, C.A.; Skvarca, P. Glacier acceleration and thinning after ice shelf collapse in the Larsen B embayment, Antarctica. *Geophys. Res. Lett.* **2004**, *31*, L18402. [CrossRef]
45. Wang, S.; Liu, H.; Jezek, K.; Alley, R.B.; Wang, L.; Alexander, P.; Huang, Y. Controls on Larsen C Ice Shelf retreat from a 60-year satellite data record. *J. Geophys. Res. Earth Surf.* **2022**, *127*, e2021JF006346. [CrossRef]
46. Cesca, S.; Sugan, M.; Rudzinski, L.; Vajedian, S.; Niemz, P.; Plank, S.; Petersen, G.; Deng, Z.; Rivalta, E.; Vuan, A.; et al. Massive earthquakes swarm driven by magmatic intrusion at the Bransfield Strait, Antarctica. *Comms. Earth Environ.* **2022**, *3*, 89. [CrossRef]
47. Fretwell, P.; Pritchard, H.D.; Vaughan, D.G.; Bamber, J.L.; Barrand, N.E.; Bell, R.; Bianchi, C.; Bingham, R.G.; Blankenship, D.D.; Casassa, G.; et al. Bedmap2: Improved ice bed, surface and thickness datasets for Antarctica. *Cryosphere* **2013**, *7*, 375–393. [CrossRef]
48. Christie, F.D.W.; Benham, T.J.; Batchelor, C.L.; Rack, W.; Montelli, A.; Dowdeswell, J.A. Antarctic ice-shelf advance driven by anomalous atmospheric and sea-ice circulation. *Nat. Geosci.* **2022**, *15*, 356–362. [CrossRef]
49. Zotikov, I.A. *Thermal Regime of the Antarctic Glacier Cover*; Gidrometeoizdat: Leningrad, Russia, 1977; 168p.
50. Lösing, M.; Ebbing, J.; Szwillus, W. Geothermal heat flux in Antarctica: Assessing models and observations by Bayesian inversion. *Front. Earth Sci.* **2020**, *8*, 105. [CrossRef]
51. Epifanov, V.P. Physical simulation of glacier motion modes. *Ice Snow* **2016**, *56*, 333–344. (In Russian) [CrossRef]
52. Lay, T.; Kanamori, H. An asperity model of large earthquake sequences. In *Earthquake Prediction: An International Review*; Simpson, D.W., Richards, P.G., Eds.; American Geophysical Union: Washington, DC, USA, 1981; pp. 579–592.
53. Leitchenkov, G.L.; Guseva, Y.B.; Gandyukhin, V.V.; Ivanov, S.V. *Structure of the Earth's Crust and Geologic Evolution History of the Sedimentary Basins of the Indian Ocean Water Area of Antarctica*; VNIIOkeangeologiya: Saint-Petersburg, Russia, 2015; 200p. (In Russian)
54. Baranov, A.; Morelli, A.; Chuvaev, A. ANTASed–An Updated Sediment Model for Antarctica. *Front. Earth Sci.* **2021**, *9*, 722699. [CrossRef]
55. Baranov, A.; Morelli. The structure of sedimentary basins of Antarctica and a new three-layer sediment model. *Tectonophysics* 2022, *in press*. Available online: https://papers.ssrn.com/sol3/papers.cfm?abstract_id=4080330 (accessed on 20 August 2022).
56. Baranov, A.; Tenzer, R.; Morelli, A. Updated Antarctic Crustal Model. *Gondwana Res.* **2021**, *89*, 1–18. [CrossRef]
57. Baranov, A.; Tenzer, R.; Bagherbandi, M. Combined Gravimetric-Seismic Crustal Model for Antarctica. *Surv. Geophys.* **2018**, *39*, 23–56. [CrossRef]
58. Baranov, A.; Morelli, A. The Moho depth map of the Antarctica region. *Tectonophysics* **2013**, *609*, 299–313. [CrossRef]
59. Domack, E.; Ishman, S.; Leventer, A.; Sylva, S.; Willmott, V.; Huber, B. A chemotrophic ecosystem found beneath Antarctic Ice Shelf. *EOS Trans. AGU* **2005**, *86*, 269–272. [CrossRef]
60. Wadham, J.L.; Arndt, S.; Tulaczyk, S.; Stibal, M.; Tranter, M.; Telling, J.; Lis, G.P.; Lawson, E.; Ridgwell, A.; Dubnick, A.; et al. Potential methane reservoirs beneath Antarctica. *Nature* **2012**, *488*, 633–637. [CrossRef]
61. Thurber, A.R.; Seabrook, S.; Welsh, R.M. Riddles in the cold: Antarctic endemism and microbial succession impact methane cycling in the Southern Ocean. *Proc. Biol. Sci.* **2020**, *287*, 20201134. [CrossRef]
62. Wille, J.D.; Favier, V.; Jourdain, N.C.; Kittel, C.; Turton, J.V.; Agosta, C.; Grodetskaya, I.V.; Picard, G.; Codron, F.; Leroy-Dos Santos, C.; et al. Intense atmospheric rivers can weaken ice shelf stability at the Antarctic Peninsula. *Comms. Earth Environ.* **2022**, *3*, 90. [CrossRef]